JCI The Journal of Clinical Investigation

Dengue virus induces PCSK9 expression to alter antiviral responses and disease outcomes

Esther S. Gan, … , Eng Eong Ooi, Sophie Yacoub

J Clin Invest. 2020. https://doi.org/10.1172/JCI137536.

Research In-Press Preview **Infectious disease**

Graphical abstract

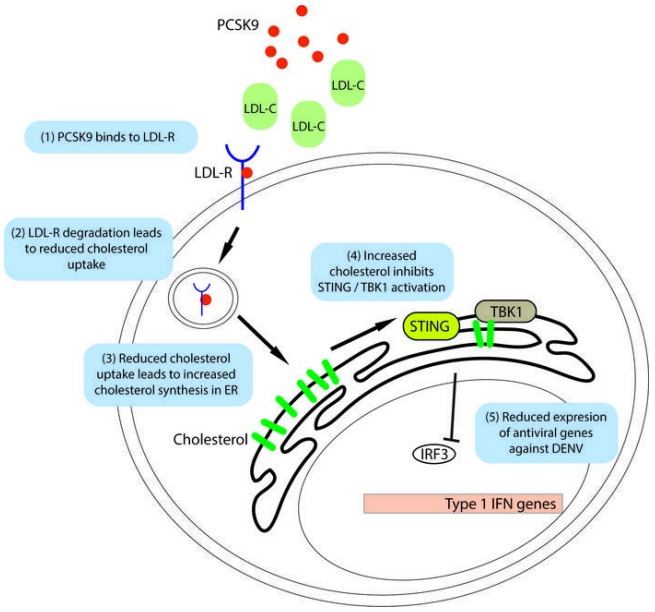

Dengue virus induces PCSK9 expression to alter antiviral responses and disease outcomes

Esther Shuyi Gan[1], Hwee Cheng Tan[1], Duyen Huynh Thi Le[2], Trieu Trung Huynh[2], Bridget Wills[2,3], Nabil G. Seidah[4], Eng Eong Ooi*[1,5,6,7], Sophie Yacoub*[2,3,7]

[1]Duke-NUS Medical School, Singapore
[2]Oxford University Clinical Research Unit (OUCRU), Ho Chi Minh City, Vietnam
[3]Centre for Tropical Medicine and Global Health, University of Oxford, UK
[4] Laboratory of Biochemical Neuroendocrinology, Montreal Clinical Research Institute (IRCM; affiliated to the Université de Montréal), Montreal, QC, Canada
[5]Saw Swee Hock School of Public Health, National University of Singapore, Singapore
[6]SingHealth Duke-NUS Global Health Institute, Singapore
[7]Singapore MIT Alliance in Research and Technology, Antimicrobial Resistance Interdisciplinary Research Group, Singapore

Corresponding Authors*
Sophie Yacoub
Oxford University Clinical Research Unit, Hospital for Tropical Diseases
764 Vo Van Kiet street, District 5
Ho Chi Minh City, Vietnam
Tel: +84 28 39237954

Eng Eong Ooi
8 College Road, Singapore 169857
Tel: 6516 8594
Email: engeong.ooi@duke-nus.edu.sg

Conflict of interest statement:
The authors have declared that no conflict of interest exists

Abstract

Dengue virus (DENV) infection requires cholesterol as a pro-viral factor although statin treatment did not show antiviral efficacy in dengue patients. Here, we show that DENV infection manipulates cholesterol metabolism in cells residing in low oxygen microenvironments (hypoxia) such as the liver, spleen and lymph nodes. DENV infection induced proprotein convertase subtilisin/kexin type 9 (*PCSK9*), which reduces low-density lipoprotein receptor (*LDLR*) recycling and hence cholesterol uptake. We found that, whereas *LDLR* uptake would have distributed cholesterol throughout the various cell compartments, de novo cholesterol synthesis enriched this lipid in the endoplasmic reticulum (ER). With cholesterol enrichment in the ER, ER-resident STING and type-I interferon (*IFN*) activation were repressed during DENV infection. Our in vitro findings were further supported by the finding of elevated plasma *PCSK9* levels in dengue patients with high viremia and increased severity of plasma leakage. Our findings thus suggest *PCSK9* plays a hitherto unrecognized role in dengue pathogenesis and could be a suitable host-directed treatment for dengue patients.

Keywords: PCSK9, Dengue, Cholesterol, Hypoxia

Introduction

Dengue is a major global health problem. Transmitted by the urban-adapted *Aedes* mosquitoes, an estimated 390 million people are infected with one of the four types of dengue virus (DENV) annually(1). Infection presents with a range of clinical outcomes, from asymptomatic infection to self-limiting but debilitating acute febrile illness to severe dengue characterized by hypovolemic shock from vascular leakage, organ dysfunction and internal bleeding(2). If not properly managed, severe dengue can result in a mortality rate of up to 20%(3). Dengue prevention thus far has relied on vector population suppression, which when conducted comprehensively is costly and lack long-term sustainability(4). A dengue vaccine, Dengvaxia®, has been licensed although it is only indicated in those who have had a prior DENV infection; Dengvaxia® paradoxically enhances DENV infection in those who are immunologically naïve at vaccination and can thus only be given to those who have evidence of prior dengue infection(5). No licensed antiviral drug is available to treat dengue. These limitations collectively hamper our ability to reduce the global burden of dengue.

Functional genomics and studies on dengue pathogenesis have identified host factors which DENV depends on for successful infection(6-10). These findings have collectively raised the possibility of repurposing licensed inhibitors of such host factors as antiviral therapies. Such a strategy would reduce the long lead time and cost associated with new drug discovery. One such host factor is cholesterol. DENV interacts with host cellular membranes for multiple and critical steps of its lifecycle -- viral entry, fusion and replication(11). Composition of cellular membranes, especially the cholesterol content, has thus been found to impact DENV infection. Previous in vitro studies have shown that DENV stimulates host cells to increase synthesis of intracellular cholesterol by upregulating the enzymatic activity of 3-hydroxy-3-methylglutaryl-coenzyme A (*HMG-CoA*) reductase(12). As de novo cholesterol synthesis occurs in the endoplasmic reticulum (ER)(13), cholesterol aids in re-structuring the ER to enable the formation of replication complexes where DENV reproduces(11). Reducing de novo cholesterol synthesis by using statins to inhibit the rate-limiting HMG-CoA reductase activity therefore reduced DENV infection, both in vitro(14, 15) and in animal models(16). Despite these promising pre-clinical findings, however, a clinical trial of a HMG-CoA reductase inhibitor, lovastatin failed to show

useful benefit in dengue patients(17). This negative clinical trial finding thus questions the clinical validity of the laboratory findings.

The discrepant outcome between laboratory-based studies and clinical trial may be due to oxygen and its impact on cholesterol metabolism. DENV replicates in the liver, spleen and lymph nodes(18-21). These organs are known to have lower oxygen levels (~3-5% oxygen) as a consequence of the circulatory anatomy(22). Reduced oxygenation would alter cholesterol homeostasis(23) although how such altered cholesterol homeostasis affects DENV infection and pathogenesis is unknown. Such hypoxia-driven changes in cholesterol homeostasis may underpin the lack of efficacy of statin as an anti-dengue drug. Therefore, further investigations into these hypoxia-driven changes during dengue infection can provide alternative therapeutic targets such as proprotein convertase subtilisin/kexin type 9 (*PCSK9*), a key regulator of cholesterol metabolism(24).

Herein, we show that DENV infection induces the expression of *PCSK9*, a negative regulator of LDL-receptor (*LDLR*). Increased *PCSK9* levels in hypoxic cells reduces *LDLR* and hence LDL-cholesterol uptake, which further drives de novo cholesterol synthesis. Whereas *LDLR* cholesterol uptake would have distributed cholesterol throughout the cell, de novo cholesterol synthesis enriched ER-cholesterol levels that suppressed phosphorylation of stimulator of interferon gene (*STING*) and tank binding kinase (*TBK*) despite DENV infection. Reduced STING and TBK activation in turn lowered the expression of type-I interferon (*IFN*) and the downstream antiviral IFN-stimulated genes (*ISG*s). These in vitro findings were supported by clinical data that showed a direct correlation between plasma levels of *PCSK9* with higher viremia levels and disease severity in dengue patients. These findings suggest *PCSK9* as a host factor for DENV in target cells resident in hypoxic microenvironments and that inhibiting *PCSK9*(25) rather than just *HMGCoA* reductase could be a useful approach to fill the therapeutic void against dengue.

Results

DENV alters LDLR and PCSK9 expression under hypoxic conditions

DENV has been found to infect and replicate in myeloid-derived cells in lymph nodes and the spleen as well as in hepatocytes(26). All these organs have hypoxic

121 microenvironments. We have previously observed that monocytes cultured at 3% O_2
122 resulted in increased DENV infection(27). As liver-derived Huh-7 cells are more
123 susceptible to in vitro DENV infection than monocytic cell lines, we first sought to
124 determine the response of Huh-7 cells to incubation at 5% O_2. In uninfected cells,
125 incubation at 5% oxygen (hereon referred to as hypoxia) for 24 hours produced the
126 known transcriptional response to hypoxia and corresponding changes in cholesterol
127 metabolism. We found increased expression of hypoxia-induced genes such as
128 adrenomedullin (*ADM*), vascular endothelial growth factor (*VEGF*) and glucose
129 transporter 1 (*GLUT1*)(28)(Supplementary Figure 1A-C) in Huh7 cells incubated in
130 hypoxic compared to normoxic conditions. With DENV infection, hypoxic Huh7 cells
131 produced higher DENV plaque titers compared to normoxic cells (Figure 1A-B),
132 suggesting that hypoxia induced pro-viral changes in Huh-7 cells as well.
133
134 Hypoxia has previously been shown to alter cholesterol metabolism pathways(29). In
135 uninfected Huh-7 cells, the expression of *SREBP2*, the master regulator of sterol
136 synthesis was upregulated, as expected(29, 30), when incubated under hypoxic
137 compared to normoxic conditions (Figure 1C). Likewise, the SREBP2-regulated *LDLR*
138 (Figure 1D-E) was similarly induced in hypoxic Huh-7 cells and resulted in increased
139 LDL uptake (Figure 1F). The negative regulator of *LDLR*, P*CSK9* was also induced
140 (Figure 1G-H), likely to ensure tight regulation of intracellular cholesterol levels(31, 32).
141
142 Upon DENV infection, *SREBP2* expression was further augmented in hypoxic Huh-7
143 cells (Figure 2A). However, DENV infection under hypoxic conditions resulted in
144 significantly reduced plasma membrane *LDLR* levels and LDL at 24 hours post-
145 infection (Figure 2B-C). In contrast, DENV infected cells showed further increase in
146 *PCSK9* secretion (Figure 2D). As *LDLR* expression can be altered at post translational
147 stages via its negative regulator *PCSK9*(31-33), we examined if reduced *LDLR* was
148 due to the function of increased *PCSK9* secretion. We treated cells with alirocumab,
149 a therapeutic monoclonal antibody against PCSK9(34, 35). Compared to mock-treated
150 cells, alirocumab treatment restored plasma membrane levels of *LDLR* in DENV
151 infected cells (Figure 2E) and resulted in lower DENV plaque titers 24 and 48 hours
152 post infection (hpi) (Figure 2F-G). These findings collectively suggest that while
153 cholesterol uptake through increased *LDLR* occurred as expected in Huh7 cells

incubated under hypoxic conditions, DENV infection downregulated *LDLR* protein via increased expression of *PCSK9*.

PCSK9 augments DENV infection in Huh7 cells

To further define the role *PCSK9* plays in DENV infection, we supplemented Huh7 cell cultures with recombinant *PCSK9* prior to infection. The *PCSK9* concentration that maximally reduced *LDLR* levels was determined by incubating cells with a range of *PCSK9* concentrations for 24 hours (Supplementary Figure 2A). We found that 400ng/ml of *PCSK9* resulted in maximal decrease of plasma membrane *LDLR* expression under hypoxic conditions. As expected, *PCSK9* supplementation increased *SREBP2* expression at 6hpi in DENV-infected Huh-7 cells (Figure 2H), resulting in increased DENV plaque titers at 24 hpi (Figure 2I) and 48hpi (Figure 2J). This effect could be inhibited with the addition of alirocumab (Figure 2I-J) in a dose dependent manner that reduces *LDLR* expression (Supplementary Figure 2B). However, the effect of *PCSK9* on DENV infection is specific to hypoxic cells as similar supplementation experiment in normoxic Huh-7 cells did not result in similar outcomes (Supplementary Figure 2C). *PCSK9* induced increase in DENV infection was not limited to DENV2 infection as similar findings were also observed with DENV1, DENV3 and DENV4 (Supplementary Figure 3A-C). Collectively, these results indicate that *PCSK9* reduces LDLR-mediated cholesterol uptake in DENV-infected hypoxic cells.

Increased PCSK9 activity may account for lack of antiviral efficacy of statins

Our finding of *PCSK9*-mediated reduction in *LDLR* levels, in a background of hypoxia-induced *SREBP2* expression also suggest that cholesterol synthesis in DENV-infected cells could be further increased. This may have rendered standard doses of statins ineffective. To test this possibility, we first treated Huh7 cells with simvastatin or mevastatin, with and without *PCSK9* supplementation. At normoxia, non-toxic doses (Supplementary Figure 4A-B) produced no difference in EC_{50} between *PCSK9* supplemented and non-supplemented cells (Figure 2K, Supplementary Figure 4C,E). At hypoxia, however, *PCSK9* supplementation reduced the potency of both simvastatin and mevastatin in reducing DENV titers (Figure 2K, Supplementary Figure 4D,F).

PCSK9 augments DENV infection in primary myeloid cells

As myeloid cells are primary targets of DENV, we next determined if the above findings can be replicated in primary human monocytes and monocyte-derived dendritic cells (MoDC). At 3% O_2, which more closely simulates the O_2 microenvironment of lymph nodes(36), Supplementation of primary monocytes and MoDCs produced higher DENV titers following infection (Figure 3A-B). Gene expression analyses of DENV-infected, PCSK9-supplemented primary monocytes using the 250-gene human inflammation panel on the Nanostring nCounter platform revealed 7 marginally upregulated and 23 significantly downregulated genes (Figure 3C). GO biological pathway analysis identified a significant downregulation of the nuclear factor kappa-light chain enhanced of activated B cells (*NFkB*) and interferon (*IFN*) pathways (Figure 3D). These findings suggest that supplementation of PCSK9 dampens antiviral response against DENV, which could account for the observed increase in DENV replication. These changes in DENV replication (Figure 3E-F) and antiviral responses such as IFNβ and C-X-C motif chemokine 10 (*CXCL10*) (Figure 3G-H) were abrogated with the addition of alirocumab, indicating that these effects are specific to increases in *PCSK9* concentrations. Collectively, our findings suggest that increased *PCSK9* expression augments DENV infection in human myeloid-derived cells by reducing antiviral responses under low oxygen conditions representative of lymph node microenvironments.

PCSK9 suppresses STING activation and downstream antiviral response

The above findings suggest that DENV derives replicative advantage from PCSK9-mediated cellular responses. A clue for what these responses could be came from a recent study that showed increased *STING* and *TBK* activation upon reduced cholesterol levels in the ER(37). Since ER cholesterol enrichment is dependent on *de novo* cholesterol synthesis(38) whereas LDLR-mediated uptake distributes cholesterol throughout the cell(39), we hypothesized that DENV depends on *de novo* cholesterol synthesis to inhibit *STING* and *TBK* activation.

To determine if *de novo* cholesterol resulted in enriched ER cholesterol levels, we fragmented hypoxic, *PCSK9* supplemented and non-supplemented Huh7 cells and isolated ER. While total cellular cholesterol levels were similar in cells grown under both conditions (Figure 4A), ER cholesterol levels were enriched in hypoxic, PCSK9

supplemented cells (Figure 4B). We next examined the impact of cholesterol enrichment in the ER on *STING* and *TBK* activation. At baseline, *PCSK9* supplementation did not result in significant differences in *STING*, phosphorylated *STING*, *TBK* or phosphorylated *TBK* levels (Figure 4C-D). With DENV infection, however, levels of both phosphorylated *STING* and *TBK* were significantly lower at 6 hpi in PCSK9 supplemented Huh7 cells compared to non-supplemented controls (Figure 4C,E). *STING* and *TBK* activation are known to phosphorylate and activate interferon regulatory factor 3 (IRF3), leading to induction of type-I IFN activation. Indeed, *PCSK9* supplementation to Huh7 cells reduced expression of *IFNb* and *IFN* stimulated genes (ISGs), such as *CXCL10* and *MX1*, which were all reversed with the addition of alirocumab (Supplementary Figure 5A-C). Collectively, this data suggests *PCSK9* expression reduces LDLR-mediated cholesterol uptake to induce de novo cholesterol synthesis that enriches ER cholesterol levels that impairs STING-mediated type-I IFN induction.

Plasma PCSK9 concentrations increased in severe dengue patients

To verify that our *in vitro* findings are clinically pertinent, we examined the association between plasma *PCSK9* levels, DENV viremia and disease severity in a nested case-control study using a previously described prospectively enrolled cohort of dengue patients(40). A total of 314 patients with suspected dengue were enrolled at 2 Vietnamese hospitals, either as outpatients with less than 72 hours of fever or after hospitalization. Of these, 263 were laboratory-confirmed dengue cases(40) (Table 1). A subset of 111 individuals, with good clinical and basic laboratory data (serial measurements of platelet, white blood cell, neutrophil and lymphocyte counts in whole blood, serum aspartate aminotransferase (AST), alanine transaminase (ALT) as well as plasma viremia, as measured by quantitative RT-PCR at enrollment) and availability of residual plasma for*PCSK9* measurements, were included in this analysis. *PCSK9* levels in each patient were measured at 3 time-points (1-3 days post illness onset, 4-6 days post illness onset and at convalescence, 10-14 days post illness onset) (Table 2). Patients were classified into three pre-defined categories of increasing disease severity in terms of plasma leakage: Grade 0 patients had no evidence of leakage; grade 1 with 15-20% increase in haematocrit (HCT) and/or fluid accumulation and; grade 2 patients developed severe leakage including >20% HCT increase, dengue shock syndrome (DSS) or compromised respiratory function.

Relevant clinical details of the 111 patients analysed in this study is shown in Table 1. Consistent with previous findings, platelet count was significantly lower in patients with grade 2 compared to grade 0 plasma leakage at 4-6 days post illness onset, which is around the period of fever defervescence when signs of severe dengue commonly manifest (Figure 5A).

Plasma *PCSK9* levels at illness days 1-3 were similar among all patients (Table 2). However, mean levels of PCSK9 in patients with grade 0, 1 and 2 dengue at illness days 4-6 post illness onset, were 46.11ng/ml, 95.76ng/ml and 145.8ng/ml, respectively, indicating elevated *PCSK9* levels in patients with more severe disease (Figure 5B). Plasma *PCSK9* concentration negatively correlated with platelet counts (Figure 5C) and positive correlated with viremia levels (Figure 5D) at this time point. Collectively, these findings indicate that elevated *PCSK9* expression is associated with higher viremia and increased risk of more severe plasma leakage in dengue patients.

Discussion

Cholesterol plays pro-viral roles in DENV infection. Previous studies have shown that cholesterol is required for efficient DENV replication and egress. The lack of efficacy in the use of statin as an antiviral treatment against dengue was thus unexpected and underscores the need for a more detailed and clinically pertinent understanding of the interaction between DENV and cellular cholesterol.

This study highlights a hitherto unrecognised role of *PCSK9* in shaping cholesterol homeostasis in hypoxic cells to favour DENV infection. DENV infection in low oxygen microenvironments upregulates the expression and secretion of PCSK9, a negative regulator of *LDLR*. Without *PCSK9*, LDLR/LDL-C complexes are internalized via endocytosis. The acidic pH of endosomes releases LDL-C and induces a conformational change in the extracellular domain of *LDLR*, aiding in its recycling to the plasma membrane(41). *PCSK9* however, binds and inhibits this conformational change in *LDLR*, preventing its recycling. In such an instance, *LDLR* is routed to lysosomes for degradation, thus lowering its surface expression levels(42) and plasma cholesterol uptake.

With reduced *LDLR* through the increased activity of *PCSK9*, *SREBP2* would be further induced to drive expression of cholesterol biosynthesis enzymes(38, 43). Cholesterol synthesis occurs and accumulates in the ER before its distribution to subcellular pools, including the plasma membrane. Our data suggests that increased *de novo* cholesterol synthesis resulted in cholesterol enrichment in the ER that inhibits ER-resident *STING* and *TBK* activation and hence downstream type-I IFN responses. Furthermore, we demonstrate that upregulation of cholesterol synthesis by PCSK9-dependent reduction in LDLR-mediated cholesterol uptake could have, at least in part, reduced the anti-DENV efficacy of statins(15). Thus, we suggest that the subcellular localization of cholesterol rather than total cellular cholesterol level is the pro-viral determinant of DENV infection.

Whilst we have used alirocumab to demonstrate a functional role for *PCSK9* in DENV infection, our findings do suggest an anti-dengue potential for anti-PCSK9 inhibitors. PCSK9 inhibitors have been developed primarily as an alternative therapeutic approach for hypercholesterolemia. Two anti-PCSK9 mAbs, alirocumab (Praluent,

Sanofi/Regeneron Pharmaceuticals Inc.)(34, 44) and evolucumab (Repatha, Amgen Inc)(45, 46) have been licensed as treatments to lower plasma cholesterol. Both alirocumab and evolucumab are fully humanized monoclonal antibodies that bind to free plasma PCSK9 and promote the degradation of its target. Reduced *PCSK9* levels allow *LDLR* to be recycled back to the plasma membranes after endocytosis thereby increasing its expression. Clinically both antibodies have shown remarkable efficacy in reducing both plasma *PCSK9* and cholesterol levels(45, 47).

Given the possibility that *PCSK9* inhibitors could be re-purposed as anti-dengue therapy, we thus sought to establish an association between plasma *PCSK9* levels and disease severity in dengue patients. Viremia and NS1 antigenemia levels have been observed to be directly correlated of dengue severity(48-52). Greater viral and NS1 antigen burden during infection both directly and indirectly through pro-inflammatory responses are thought to compromise the integrity of the vascular endothelium, leading to plasma leakage(53-55). That plasma *PCSK9* levels directly correlated with viremia levels and extent of plasma leakage as well as negatively correlated with platelet count collectively suggest that our in vitro findings are clinically pertinent and that *PCSK9* is involved in clinical pathogenesis. Re-purposing PCSK9 inhibitors, either on their own or in conjunction with statins, could thus be an expedient approach to fill the therapeutic void against dengue.

While our study highlights an important role that *PCSK9* plays in DENV infection, a limitation in our study is the concentrations of recombinant *PCSK9* (rPCSK9) supplemented in in vitro experiments. Concentrations of 400ng/ml *PCSK9* supplemented in vitro is higher than the levels of plasma *PCSK9* observed in our clinical trial cohort. This difference can be attributed to the lower efficacy of recombinant *PCSK9* compared to the activity of *PCSK9* in vivo. There are several explanations for this effect. Firstly, in vivo, *PCSK9* undergoes several post-translational modifications such as Ser-phosphorylation by *FAM20C*. This increases *PCSK9* binding affinity to LDLR. In vitro, there is an absence of phosphorylation by *FAM20C* in rPCSK9, which reduces *PCSK9* ability to degrade *LDLR*(56). Secondly, high levels of cyclase-associated protein 1 (*CAP1*) are present in the liver as compared to in vitro conditions. *CAP1* has been shown to bind to *PCSK9* to mediate

endocytosis and lysosomal degradation of *LDLR*. Thus, lower levels of *CAP1* in vitro reduces the activity of *PCSK9*(57). Thus, concentrations of *PCSK9* supplemented in vitro cannot be compared to plasma *PCSK9* levels.

Our molecular studies have been focused on DENV-targeted cells. The interpretation of cholesterol homeostasis at a systemic level in dengue patients is likely more complex. Reduced circulating LDL-C has been associated with severe dengue patients(58). Our *PCSK9* finding also suggests that reduced plasma LDL-C in severe dengue patients is not due to increased LDL-C uptake. Instead, it is possible that impaired cholesterol synthesis in the liver, which is known to be inflamed in severe dengue patients(59), could have lowered cholesterol production. Alternatively, increased endothelial permeability associated could also have resulted in leakage of cholesterol molecules into the extravascular space and thus lowered plasma LDL-C levels(60, 61). Further studies will be needed to tease these possibilities apart.

Our study also has implications on dengue pathogenesis investigations. DENV infects myeloid cells in the lymph nodes, the spleen and liver where the microenvironments are physiologically hypoxic. Inflammation such as those triggered by infection, including DENV can exacerbate hypoxia in these microenvironments as generation of reactive oxygen species depletes O_2 levels further(62). That *PCSK9* plays an important role in DENV infection under such low O_2 conditions could thus not have been gleaned from conventional experimental studies on dengue that incubate virus and cells at ambient O_2 levels. Likewise, the role of *PCSK9* could also not have been deciphered in mouse studies. Mouse plasma cholesterol is transported in high density lipoprotein (HDL) instead of LDL. The uptake of cholesterol in mice is thus not dependent on *LDLR*(63, 64). *PCSK9* would thus not have a significant impact in dengue pathogenesis in a mouse model.

In conclusion, our findings show how cholesterol metabolism in cells that reside in organs with low oxygen concentrations is altered upon DENV infection to facilitate pathogenesis. Importantly, it suggests that inhibition of *PCSK9* activity using an inhibitory mAb or RNA interference approaches(25) could be safe therapeutic approaches for dengue patients.

Material and Methods

Cells: Huh7, BHK-21 and Vero cells were obtained from the American Type Culture Collection (ATCC) and cultured in DEME media (Gibco) supplemented with 9% fetal calf serum (HyClone). Both cells lines tested negative for mycoplasma. When required, cells were adapted to 5% O_2 in a fully humidified incubator supplied with 5% CO_2 as well as nitrogen gas to reduce oxygen levels for 24 hours prior to infection with DENV2.

Monocytes and monocytes derived dendritic cells (moDC): Peripheral blood mononuclear cells (PBMC) were isolated from a flavivirus naïve healthy donor, under a protocol approved by the National University of Singapore Institutional Review Board (IRB B-15-227). CD14+ monocytes were isolated from PBMCs using CD14 microbeads (Miltenyl Biotec 130-050-201) according to the manufacturers protocol. To obtain moDCs, monocytes were cultured in 6 well tissue culture plates and supplemented with growth media (RPMI-1640, 10% FBS, 100U/ml penicillin, 100ug/ml streptomycin) containing 100ng/ml of IL-4 (eBioscience) and 50ng/ml of granulocyte macrophage-colony stimulating factor (GM-CSF).

Virus infection and plaque assays: DENV2 (ST) is a clinical isolate obtained from Singapore General Hospital and passaged 6 times in Vero cells. DENV1-2402, DENV3-863, DENV4-2270 are clinical isolates obtained from a previous clinical trial. For Huh7 infections, cells were infected with DENV for 2 hours at 37^{o}C at MOI:1. Virus inoculum was then removed. After infection, cells are maintained in DMEM media containing 9% FBS. Primary monocytes were infected with DENV-2 at MOI:10 for the duration of the experiment. moDC were infected with DENV-2 at MOI:1 for the duration of the experiment. Supernatants were collected at the specified time point and stored at -80^{0}C prior to plaque assay quantification. Plaque assay was performed on BHK-21 cells using maintenance media with RPMI 1640 as previously described(65).

q-PCR: RNA from cells were extracted with RNeasy Kit (Qiagen) followed by cDNA synthesis (QuantaBio) and real-time qPCR with SYBR (Roche) according to manufacturer's protocol. All RNA levels were measured relative to TATA-box binding protein (TBP). Primer sequences used are as follows:

DENV-Forward TTGAGTAAACYRTGCTGCCTGTAGCTC,

DENV-Reverse GAGACAGCAGGATCTCTGGTCTYTC

TBP-Forward TGTATCCACAGTGAATCTTGGTTG

TBP-Reverse GGTTCGTGGCTCTCTTATCCTC

LDLR-Forward GAATCTACTGGTCTGACCTGTCC

LDLR-Reverse GGTCCAGTAGATGTTGCTGTGG

PCSK9-Forward GACACCAGCATACAGAGTGACC

PCSK9-Reverse GTGCCATGACTGTCACACTTGC

SREBP2-Forward CTCCATTGACTCTGAGCCAGGA

SREBP2-Reverse GAATCCGTGAGCGGTCTACCAT

GLUT1-Forward TTGCAGGCTTCTCCAACTGGAC

GLUT1-Reverse CAGAACCAGGAGCACAGTGAAG

IFNβ-Forward CTTGGATTCCTACAAAGAAGCAGC

IFNβ-Reverse TCCTCCTTCTGGAACTGCTGCA

CXCL10-Forward GGTGAGAAGAGATGTCTGAATCC

CXCL10-Reverse GTCCATCCTTGGAAGCACTGCA

LDLR Flow cytometry: After oxygen adaptation or DENV2 infection, cells were dissociated with Accutase (Stemcell technologies 07920), washed with phosphate buffer solution (PBS) and fixed with 3% paraformaldehyde at 4^{o}C for 30mins. Mouse anti LDLR (1:300, R&D) was then added for 30 mins at 4^{o}C. After further washing with PBS, anti-mouse Alexa-Fluor 647 (1:400) was added and incubate at 4^{o}C for 30 mins prior to analysis with the BD LSRFortessa flow cytometer.

DIL-LDL: DIL labelled low density lipoprotein (Thermofisher L3482) was diluted in serum free DMEM to a concentration of 1ug/ml. After oxygen adaptation or DENV2 infection, Huh7 cells were washed with PBS prior to addition of 1ug/ml of DIL-LDL. Cells are then incubated at 37^{o}C for 3 hours, washed in PBS and fixed in 3% PFA for 30 mins prior to FACS analysis.

Alirocumab: Praluent (Sanofi US and Regeneron Pharmaceuticals),150mg/ml (alirocumab) was used for the experiments. . The drug was stored at 4^{o} and diluted to a working concentration of 1μM in DMEM.

MTS assay: CellTiter 96 AQueous One Solution Cell Proliferation Assay (MTS) was purchased from Promega (G3580). Briefly, MTS is a tetrazolium compound (3-(4,5-dimethylthiazol-2-yl)-5-(3-carboxymethoxyphenyl)-2-(4-sulfophenyl)-2H-tetrazolium)) used in a colorimetric assay to determine the number of viable cells. To assay effects of statins, Huh7 cells were seeded overnight prior to treatment with statins for 24h at 5% O_2. MTS was added for 2 hours and absorbance read at 490 nm.

Western Blot: Cells were washed once in PBS and resuspended in lysis buffer (1% Nonidet P-40, 150mM NaCl, 50mM Tris pH8.0) in the presence of protease inhibitors (1:100, Sigma). Proteins in cells lysates were denatured at 95^{O}C in loading buffer (Biorad) and 2-mercaptoethanol (1:10) prior to separation b SDS-PAGE, transferred to PVDF (Millipore) and incubated with primary antibodies followed by HRP-conjugated anti-rabbit (1:10000, Abcam 6721) or anti-mouse (1:10000, Dako P0447) antiserum. Primary antibodies for LAMP1 (1:1000, eBioscience 6721), STING (1:1000, CST 13647S), phosphoSTING (1:1000, CST 72971), TBK (1:1000, CST 3504S), phosphoTBK (1:1000, CST 5483S) and calrecticulin (1:1000, Abcam 2907) were used. Blots were developed using enhanced chemiluminescence detection reagents (Amersham). Data shown is representative of 3 independent experiments. Quantification of protein densitometry was performed with ImageJ 1.47v.

Nanostring: 50ng of extracted RNA were hybridized to the Nanostring nCounter human inflammation panel at 65^{0}C for 24 hours. Hybridized samples were quantified using the nCounter Sprint profiler (NanoString Technologies). Data was analyzed using the nSolver Analysis Software (NanoString Technologies). Subsequent pathway analysis was performed using GO Biological Pathways analysis.

ER isolation and cholesterol quantification: Isolation of ER from Huh7 cells were performed as previously described(66). Cholesterol quantification was performed using the Amplex Red Cholesterol Assay Kit (A12216, ThermoFisher Scientific) according to manufacturer's protocol. Cholesterol levels were normalized to the densitometry of calrecticulin to account for any difference in ER concentrations.

PCSK9 quantification: Huh7 cells were centrifuged at maximum speed at 4^{o}C for 10 mins to remove any cellular debris. Supernatant was stored at -80^{o}C prior to

quantification. PCSK9 quantification was performed at 1:10 dilution with Human PCSK9 ELISA Kit (Abcam, 209884) according to manufacturer's protocol.

Patient plasma PCSK9 Quantification:: Plasma concentration of PCSK9 was measured at 3 time points: enrolment, 48 hours later and follow-up 10–14 days after illness onset. These were performed at the OUCRU laboratories in Ho Chi Minh City, using a human magnetic luminex assay (Premixed Multiplex kit-LXSAHM-05) on a Luminex 200 analyzer, according to the manufacturer's specifications (R&D Systems).

Clinical Study: A nested case control study was performed using stored plasma samples from a prospective study that enrolled 316 patients from both outpatient facilities and inpatient wards, at the Hospital for Tropical Disease (HTD), Ho Chi Minh City, and the National Hospital for Tropical Diseases (NHTD), Hanoi, Vietnam(40). From this cohort we randomly selected 111 patients including 56 patients with plasma leakage (29 grade 2 and 27 grade 1) compared to 53 without evidence of leakage. Patients were included if they had sufficient plasma stored for more than 1 time-point and all the clinical data required for the plasma leak grading. Patients were classified into three pre-defined categories of increasing disease severity as indicated by plasma leakage: Grade 0 patients had no evidence of leakage; grade 1 patients had a 15-20% increase in haematocrit (HCT) and/or fluid accumulation; grade 2 patients had evidence of severe leakage including >20% HCT increase, DSS or compromised respiratory function. Dengue diagnostics for NS1 test (Platelia ELISA, Biorad), immunoglobulin serology and RT-PCR have been described in the original publication(40).

Statistical Analysis: In vitro experiments were replicated 3 times, each with a minimum of 3 biological replicates. Representative data from 1 of these 3 independent experiments are shown in the figures. 2-tailed unpaired t-test was performed to compare between the means of 2 conditions using GraphPad Prism v8.0. Statistical analysis for data sets with more than 2 groups was performed with one-way ANOVA corrected with Tukey multiple comparison test. For all data sets, P-value <0.05 was considered significant. Statistical analysis for patient clinical

parameters was performed with one-way ANOVA corrected for multiple comparisons with Dunetts test against Group 0 (control).

Study approval: Ethical approval for clinical study “An investigation into the pathophysiology of disease progression in dengue in Vietnam” was obtained from the Oxford Tropical Research Ethics Committee (Oxtrec reference: 1030-13) and the Ethics Review Committee at the National Hospital for Tropical Diseases, Ho Chi Minh City.

Author Contributions: ESG, SY and EEO designed the study. ESG and THC performed the in vitro experiments. DHTL performed the PCSK9 luminex from the Vietnamese cohort. BWSY and TTH led the clinical studies in Vietnam. ESG and EEO analyzed the data and wrote the first version of the manuscript. ESG, NGS, BW, SY and EEO reviewed and revised the manuscript.

Acknowledgements: ESG is supported by the Estate of Tan Sri Khoo Teck Puat under its Khoo Postdoctoral Fellowship Award (Duke-NUS-KPFA/2018/0023) administered by Duke-NUS Medical School. EEO is supported by the Singapore National Medical Research Foundation under its Clinician-Scientist Award administered by the National Medical Research Council. SY was supported by the Singapore National Medical Research Foundation under its Young-Investigator Research Grant (NMRC/OFYIRG/0050.2017). The clinical trial was supported by the Wellcome Trust (100562/Z/12/Z).

Author information: Correspondence and all request for materials should be addressed to engeong.ooi@duke-nus.edu.sg

References

1. Bhatt S et al. The global distribution and burden of dengue. *Nature* 2013;496(7446):504–507.

2. Wilder-Smith A, Ooi EE, Horstick O, Wills B. Dengue. *Lancet* 2019;393(10169):350–363.

3. Simmons CP, Farrar JJ, Nguyen VVC, Wills B. Dengue. *N. Engl. J. Med.* 2012;366(15):1423–1432.

4. Ooi EE, Goh K-T, Gubler DJ. Dengue Prevention and 35 Years of Vector Control in Singapore. *Emerg. Infect. Dis.* 2006;12(6):887–893.

5. Sridhar S et al. Effect of Dengue Serostatus on Dengue Vaccine Safety and Efficacy. *N. Engl. J. Med.* 2018;379(4):327–340.

6. Krishnan MN et al. Rab 5 is required for the cellular entry of dengue and West Nile viruses. *J. Virol.* 2007;81(9):4881–4885.

7. Sessions OM et al. Discovery of insect and human dengue virus host factors. *Nature* 2009;458(7241):1047–1050.

8. Le Sommer C, Barrows NJ, Bradrick SS, Pearson JL, Garcia-Blanco MA. G protein-coupled receptor kinase 2 promotes flaviviridae entry and replication.2012;6(9):e1820.

9. Savidis G et al. Identification of Zika Virus and Dengue Virus Dependency Factors using Functional Genomics. *Cell Rep* 2016;16(1):232–246.

10. Richardson RB et al. A CRISPR screen identifies IFI6 as an ER-resident interferon effector that blocks flavivirus replication. *Nature Microbiology* 2018;3(11):1214–1223.

11. Welsch S et al. Composition and Three-Dimensional Architecture of the Dengue Virus Replication and Assembly Sites. *Cell Host Microbe* 2009;5(4):365–375.

12. Soto-Acosta R, Bautista-Carbajal P, Cervantes-Salazar M, Angel-Ambrocio AH, del Angel RM. DENV up-regulates the HMG-CoA reductase activity through the impairment of AMPK phosphorylation: A potential antiviral target. *PLoS Pathog.* 2017;13(4):e1006257.

13. Afonso MS et al. Molecular Pathways Underlying Cholesterol Homeostasis. *Nutrients* 2018;10(6):760.

14. Bryan-Marrugo OL et al. The anti-dengue virus properties of statins may be associated with alterations in the cellular antiviral profile expression. *Mol Med Rep* 2016;14(3):2155–2163.

15. Martinez-Gutierrez M, Castellanos JE, Gallego-Gómez JC. Statins reduce dengue virus production via decreased virion assembly. *Intervirology* 2011;54(4):202–216.

16. Martinez-Gutierrez M, Correa-Londoño LA, Castellanos JE, Gallego-Gómez JC, Osorio JE. Lovastatin delays infection and increases survival rates in AG129 mice infected with dengue virus serotype 2. *PLoS ONE* 2014;9(2):e87412.

17. Whitehorn J et al. Lovastatin for the Treatment of Adult Patients With Dengue: A Randomized, Double-Blind, Placebo-Controlled Trial. *Clin. Infect. Dis.* 2016;62(4):468–476.

18. Nisalak A et al. Observations related to pathogenesis of dengue hemorrhagic fever. 3. Virologic studies of fatal disease. *Yale J Biol Med* 1970;42(5):293–310.

19. Balsitis SJ et al. Tropism of dengue virus in mice and humans defined by viral nonstructural protein 3-specific immunostaining. *Am. J. Trop. Med. Hyg.* 2009;80(3):416–424.

20. Basílio-de-Oliveira CA, Aguiar GR. Pathologic study of a fatal case of dengue-3 virus infection in Rio de Janeiro, Brazil. *Brazilian Journal of …* 2005;

21. Aye KS et al. Pathologic highlights of dengue hemorrhagic fever in 13 autopsy cases from Myanmar. *Hum. Pathol.* 2014;45(6):1221–1233.

22. Caldwell PRB, Wittenberg BA. The oxygen dependency of mammalian tissues. *The American Journal of Medicine* 1974;57(3):447–452.

23. Brown MS, Radhakrishnan A, Goldstein JL. Retrospective on Cholesterol Homeostasis: The Central Role of Scap. *Annu. Rev. Biochem.* 2018;87(1):783–807.

24. Seidah NG, Awan Z, Chrétien M, Mbikay M. PCSK9: a key modulator of cardiovascular health. *Circ. Res.* 2014;114(6):1022–1036.

25. Seidah NG, Prat A, Pirillo A, Catapano AL, Norata GD. Novel strategies to target proprotein convertase subtilisin kexin 9: beyond monoclonal antibodies. *Cardiovasc. Res.* 2019;115(3):510–518.

26. Aye KS et al. Pathologic highlights of dengue hemorrhagic fever in 13 autopsy cases from Myanmar. *Hum. Pathol.* 2014;45(6):1221–1233.

27. Gan ES et al. Hypoxia enhances antibody-dependent dengue virus infection. *The EMBO Journal* 2017;:e201695642.

28. Semenza GL. Targeting HIF-1 for cancer therapy. *Nature Reviews Cancer* 2003;3(10):721–732.

29. Nguyen AD, McDonald JG, Bruick RK, DeBose-Boyd RA. Hypoxia stimulates degradation of 3-hydroxy-3-methylglutaryl-coenzyme A reductase through accumulation of lanosterol and hypoxia-inducible factor-mediated induction of insigs. *Journal of Biological Chemistry* 2007;282(37):27436–27446.

30. Hwang S et al. Hypoxia-inducible factor 1α activates insulin-induced gene 2 (Insig-2) transcription for degradation of 3-hydroxy-3-methylglutaryl (HMG)-CoA reductase in the liver. *J. Biol. Chem.* 2017;292(22):9382–9393.

31. Abifadel M et al. Mutations in PCSK9 cause autosomal dominant hypercholesterolemia. *Nat. Genet.* 2003;34(2):154–156.

32. Horton JD, Cohen JC, Hobbs HH. Molecular biology of PCSK9: its role in LDL metabolism. *Trends Biochem. Sci.* 2007;32(2):71–77.

33. Dubuc G et al. Statins upregulate PCSK9, the gene encoding the proprotein convertase neural apoptosis-regulated convertase-1 implicated in familial hypercholesterolemia. *Arterioscler. Thromb. Vasc. Biol.* 2004;24(8):1454–1459.

34. Robinson JG et al. Efficacy and safety of alirocumab in reducing lipids and cardiovascular events. *N. Engl. J. Med.* 2015;372(16):1489–1499.

35. Tavori H, Melone M, Rashid S. Alirocumab: PCSK9 inhibitor for LDL cholesterol reduction. *Expert Rev Cardiovasc Ther* 2014;12(10):1137–1144.

36. Caldwell CC et al. Differential effects of physiologically relevant hypoxic conditions on T lymphocyte development and effector functions. *J. Immunol.* 2001;167(11):6140–6149.

37. York AG et al. Limiting Cholesterol Biosynthetic Flux Spontaneously Engages Type I IFN Signaling. *Cell* 2015;163(7):1716–1729.

38. Horton JD, Goldstein JL, Brown MS. SREBPs: activators of the complete program of cholesterol and fatty acid synthesis in the liver. *J Clin Invest* 2002;109(9):1125–1131.

39. Das A, Brown MS, Anderson DD, Goldstein JL, Radhakrishnan A. Three pools of plasma membrane cholesterol and their relation to cholesterol homeostasis. *Elife* 2014;3:19316.

610 40. Yacoub S et al. Endothelial Nitric Oxide Pathways in the Pathophysiology of Dengue: A
611 Prospective Observational Study. *Clin. Infect. Dis.* 2017;65(9):1453–1461.

612 41. Brown MS, Goldstein JL. Expression of the familial hypercholesterolemia gene in heterozygotes:
613 mechanism for a dominant disorder in man. *Science* 1974;185(4145):61–63.

614 42. Maxwell KN, Fisher EA, Breslow JL. Overexpression of PCSK9 accelerates the degradation of the
615 LDLR in a post-endoplasmic reticulum compartment. *PNAS* 2005;102(6):2069–2074.

616 43. Brown MS, Goldstein JL. The SREBP pathway: regulation of cholesterol metabolism by
617 proteolysis of a membrane-bound transcription factor. *Cell* 1997;89(3):331–340.

618 44. Schwartz GG et al. Alirocumab and Cardiovascular Outcomes after Acute Coronary Syndrome. *N.*
619 *Engl. J. Med.* 2018;:NEJMoa1801174.

620 45. Sabatine MS et al. Cardiovascular safety and efficacy of the PCSK9 inhibitor evolocumab in
621 patients with and without diabetes and the effect of evolocumab on glycaemia and risk of new-onset
622 diabetes: a prespecified analysis of the FOURIER randomised controlled trial. *Lancet Diabetes*
623 *Endocrinol* 2017;5(12):941–950.

624 46. Sabatine MS et al. Evolocumab and Clinical Outcomes in Patients with Cardiovascular Disease.
625 *N. Engl. J. Med.* 2017;376(18):1713–1722.

626 47. Gaudet D et al. Effect of alirocumab, a monoclonal proprotein convertase subtilisin/kexin 9
627 antibody, on lipoprotein(a) concentrations (a pooled analysis of 150 mg every two weeks dosing from
628 phase 2 trials). *Am. J. Cardiol.* 2014;114(5):711–715.

629 48. Libraty DH et al. High circulating levels of the dengue virus nonstructural protein NS1 early in
630 dengue illness correlate with the development of dengue hemorrhagic fever. *J Infect Dis.*
631 2002;186(8):1165–1168.

632 49. Avirutnan P et al. Vascular leakage in severe dengue virus infections: a potential role for the
633 nonstructural viral protein NS1 and complement. *J Infect Dis.* 2006;193(8):1078–1088.

634 50. Thomas L et al. Relationship between nonstructural protein 1 detection and plasma virus load in
635 Dengue patients. *Am. J. Trop. Med. Hyg.* 2010;83(3):696–699.

636 51. Vaughn DW et al. Dengue viremia titer, antibody response pattern, and virus serotype correlate
637 with disease severity. *J Infect Dis.* 2000;181(1):2–9.

638 52. la Cruz-Hernández de SI et al. Determination of viremia and concentration of circulating
639 nonstructural protein 1 in patients infected with dengue virus in Mexico. *Am. J. Trop. Med. Hyg.*
640 2013;88(3):446–454.

641 53. Adikari TN et al. Dengue NS1 antigen contributes to disease severity by inducing interleukin (IL)-
642 10 by monocytes. *Clinical & Experimental Immunology* 2016;184(1):90–100.

643 54. Beatty PR et al. Dengue virus NS1 triggers endothelial permeability and vascular leak that is
644 prevented by NS1 vaccination. *Science Translational Medicine* 2015;7(304):304ra141–304ra141.

645 55. Puerta-Guardo H, Glasner DR, Harris E. Dengue Virus NS1 Disrupts the Endothelial Glycocalyx,
646 Leading to Hyperpermeability. *PLoS Pathog.* 2016;12(7):e1005738.

647 56. Ben Djoudi Ouadda A et al. Ser-Phosphorylation of PCSK9 (Proprotein Convertase Subtilisin-
648 Kexin 9) by Fam20C (Family With Sequence Similarity 20, Member C) Kinase Enhances Its Ability to
649 Degrade the LDLR (Low-Density Lipoprotein Receptor). *Arterioscler. Thromb. Vasc. Biol.*
650 2019;39(10):1996–2013.

651 57. Jang H-D et al. Cyclase-associated protein 1 is a binding partner of proprotein convertase

652 subtilisin/kexin type-9 and is required for the degradation of low-density lipoprotein receptors by
653 proprotein convertase subtilisin/kexin type-9. *Eur. Heart J.* 2020;41(2):239–252.

654 58. Biswas HH et al. Lower Low-Density Lipoprotein Cholesterol Levels Are Associated with Severe
655 Dengue Outcome.2015;9(9):e0003904.

656 59. Lee LK et al. Clinical relevance and discriminatory value of elevated liver aminotransferase levels
657 for dengue severity. *PLoS Negl Trop Dis* 2012;6(6):e1676.

658 60. Trung DT, Wills B. Systemic vascular leakage associated with dengue infections - the clinical
659 perspective. *Curr. Top. Microbiol. Immunol.* 2010;338(3):57–66.

660 61. Wills BA et al. Size and charge characteristics of the protein leak in dengue shock syndrome. *J*
661 *Infect Dis.* 2004;190(4):810–818.

662 62. Campbell EL et al. Transmigrating neutrophils shape the mucosal microenvironment through
663 localized oxygen depletion to influence resolution of inflammation. *Immunity* 2014;40(1):66–77.

664 63. Camus MC, Chapman MJ, Forgez P, Laplaud PM. Distribution and characterization of the serum
665 lipoproteins and apoproteins in the mouse, Mus musculus. *J. Lipid Res.* 1983;24(9):1210–1228.

666 64. Gordon SM et al. A comparison of the mouse and human lipoproteome: suitability of the mouse
667 model for studies of human lipoproteins. *J. Proteome Res.* 2015;14(6):2686–2695.

668 65. Chan KR et al. Ligation of Fc gamma receptor IIB inhibits antibody-dependent enhancement of
669 dengue virus infection. *Proc. Natl. Acad. Sci. U.S.A.* 2011;108(30):12479–12484.

670 66. Williamson CD, Wong DS, Bozidis P, Zhang A, Colberg-Poley AM. Isolation of Endoplasmic
671 Reticulum, Mitochondria, and Mitochondria-Associated Membrane and Detergent Resistant
672 Membrane Fractions from Transfected Cells and from Human Cytomegalovirus-Infected Primary
673 Fibroblasts. *Curr Protoc Cell Biol* 2015;68(1):3.27.1–3.27.33.

674

675

Main Figures

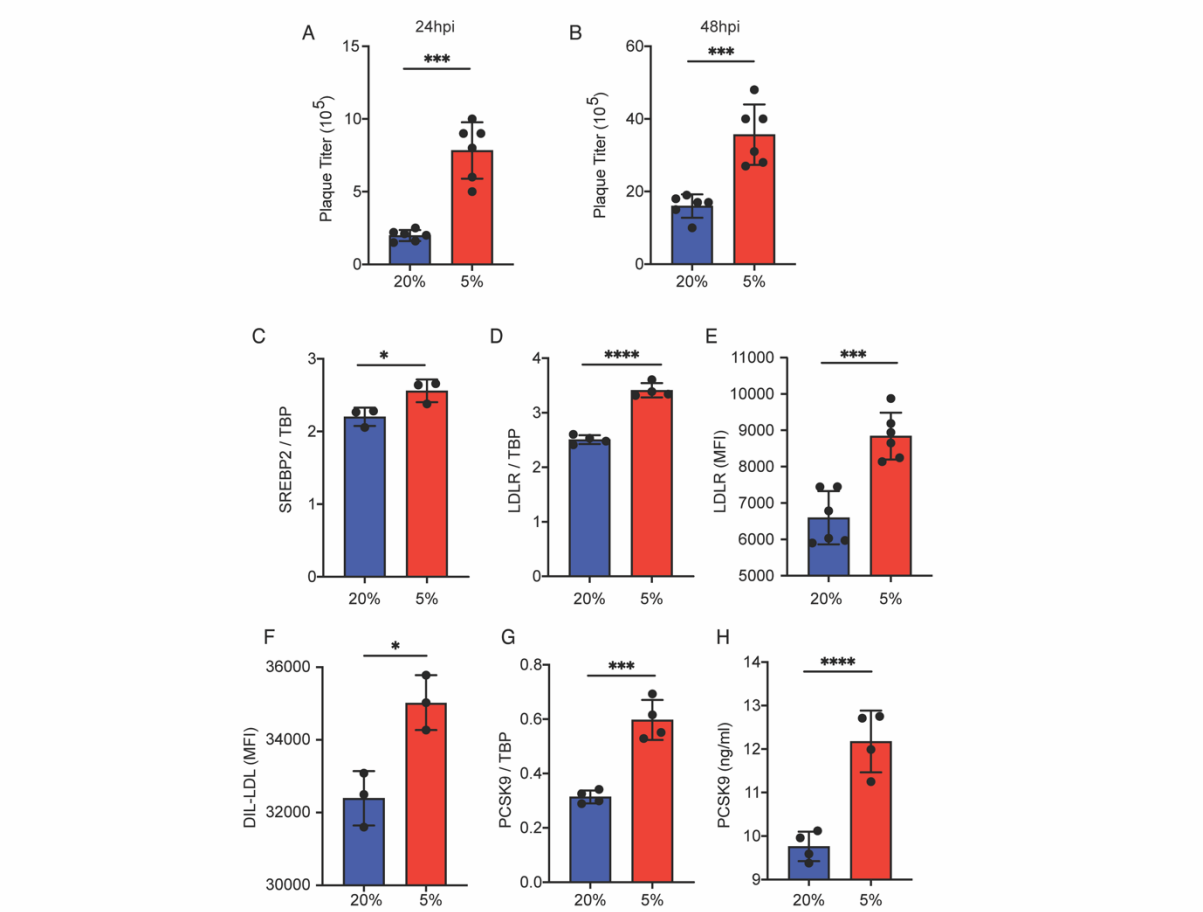

Figure 1: Hypoxia and DENV infection both alter LDLR and PCSK9 expression
(A-B) Plaque titers from normoxic (blue) and hypoxic (red) Huh7 cells at 24 (A) and 48 (B) hours post DENV2 infection. Data is expressed as plaque forming units (pfu) per ml of culture supernatant. **(C)** *SREBP2* mRNA levels in normoxic (blue) and hypoxic (red) Huh7 cells after 24 hours incubation. **(D)** *LDLR* mRNA levels in normoxic (blue) and hypoxic (red) Huh7 cells 24 hours post oxygen adaptation. **(E)** Mean fluorescence intensity (MFI) of *LDLR* in normoxic (blue) and hypoxic (red) Huh7 cells 24 hours post oxygen adaptation as assessed by flow cytometry. **(F)** Mean fluorescence intensity (MFI) of DIL-LDL in normoxic (blue) and hypoxic (red) huh7 cells 24 hours post oxygen adaptation as assessed by flow cytometry. **(G)** PCSK9 mRNA expression in normoxic (blue) or hypoxic (red) Huh7 cells 24 hours post oxygen adaptation**. (H)** Levels of secreted PCSK9 in normoxic (blue) or hypoxic (red) Huh7 cells 24 hours post oxygen adaptation as measured by ELISA. Experiments were replicated 3 times, each with a minimum of 3 biological replicates. Representative data from 1 of these 3 independent experiments are shown in the Figures. Data in (A-H) represents mean ± SD. *P<0.05, ***P<0.001, ****P<0.0001 (unpaired t-test).

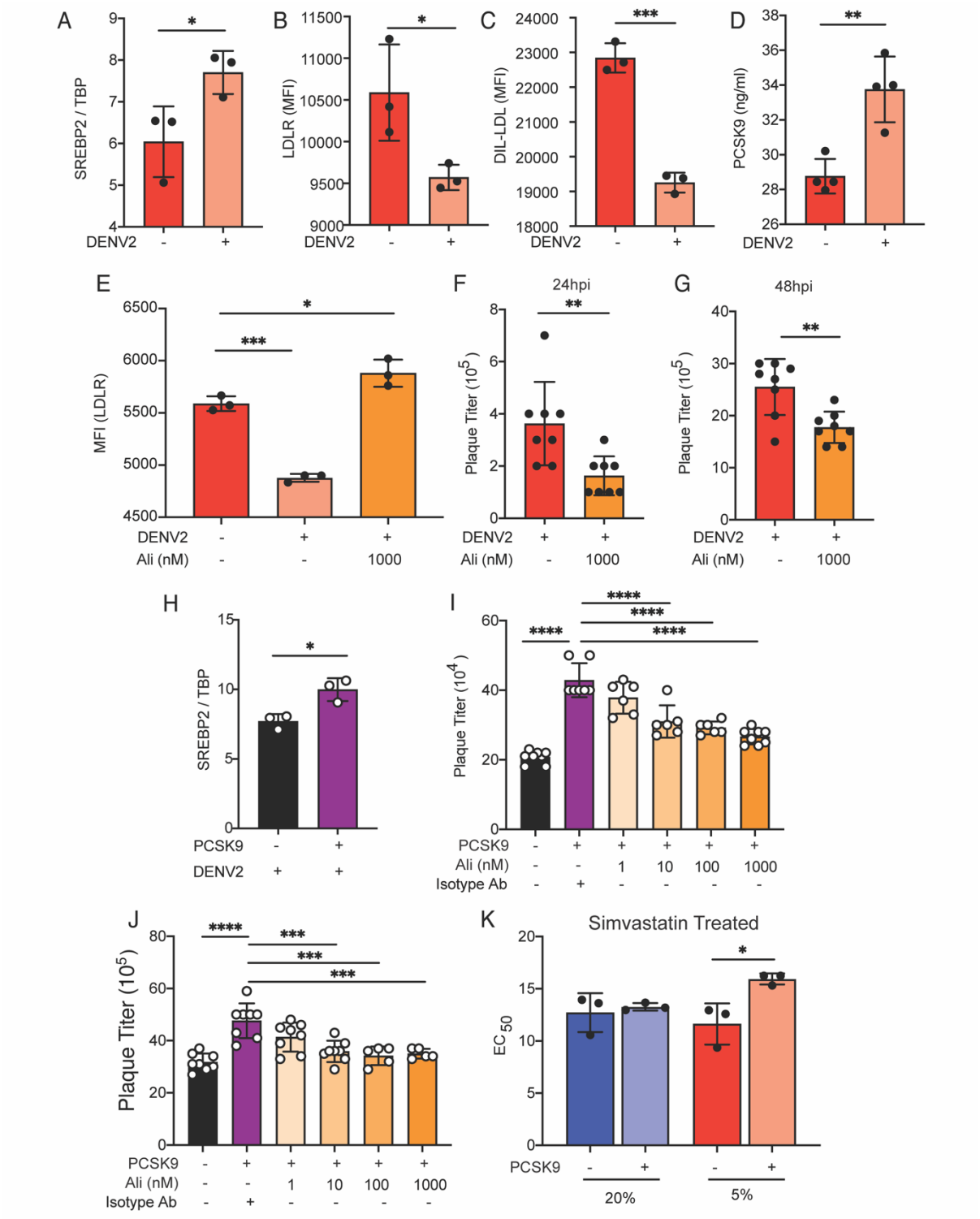

694

695 **Figure 2: PCSK9 augments DENV infection and dampens the antiviral effect of**
696 **statins**. **(A)** *SREBP2* mRNA levels in uninfected and infected hypoxic Huh7 cells 24
697 hours post-infection. **(B)** Mean fluorescence intensity (MFI) of *LDLR* in uninfected
698 and infected hypoxic Huh7 cells 24 hours post-infection as assessed by flow
699 cytometry. **(C)** Mean fluorescence intensity (MFI) of DIL-LDL in uninfected and
700 infected hypoxic Huh7 cells 24 hours post-infection as assessed by flow cytometry.
701 **(D)** Levels of secreted PCSK9 in in uninfected and infected hypoxic Huh7 cells 24
702 hours post-infection. **(E)** Mean fluorescence intensity (MFI) of LDL in uninfected,
703 infected and alirocumab treated hypoxic Huh7 cells 24 hours post-infection as

assessed by flow cytometry. **(F-G)** Plaque titers in hypoxic Huh7 cells treated with or without alirocumab 24 (F) and 48 (G) hours post infection (hpi). **(H)** mRNA expression of *SREBP2* in hypoxic Huh7 cells 6hpi. Cells were cultured without (black) or with supplementation of 400ng/ml PCSK9 (purple) 24 hours prior to DENV2 infection. **(I-J)** Plaque titers in hypoxic Huh7 cells 24 (G) and 48 (H) hpi with DENV2. Cells were cultured without (black), with supplementation of 400ng/ml PCSK9 (purple) or PCKS9 with increasing doses of alirocumab (orange) for 24 hours prior to DENV2 infection. **(K)** EC50 values of hypoxic (red) and normoxic (blue) Huh7 cells 48hpi with DENV2 treated with varying doses of simvastatin. Cells were cultured without (Dark blue, Dark red) or with supplementation of 400ng/ml PCSK9 (Light blue, Light red) 24 hours prior to DENV2 infection. Experiments were replicated 3 times, with minimum of 3 biological replicates. Representative data from 1 of these 3 independent experiments are shown in the Figures. Data in (A-D, F-H) was compared by unpaired t-test and (E, I-K) by one-way ANOVA corrected for multiple comparisons. Data in (A-K) represents mean ± SD. *P<0.05, **P<0.01, ***P<0.001, ****P<0.0001.

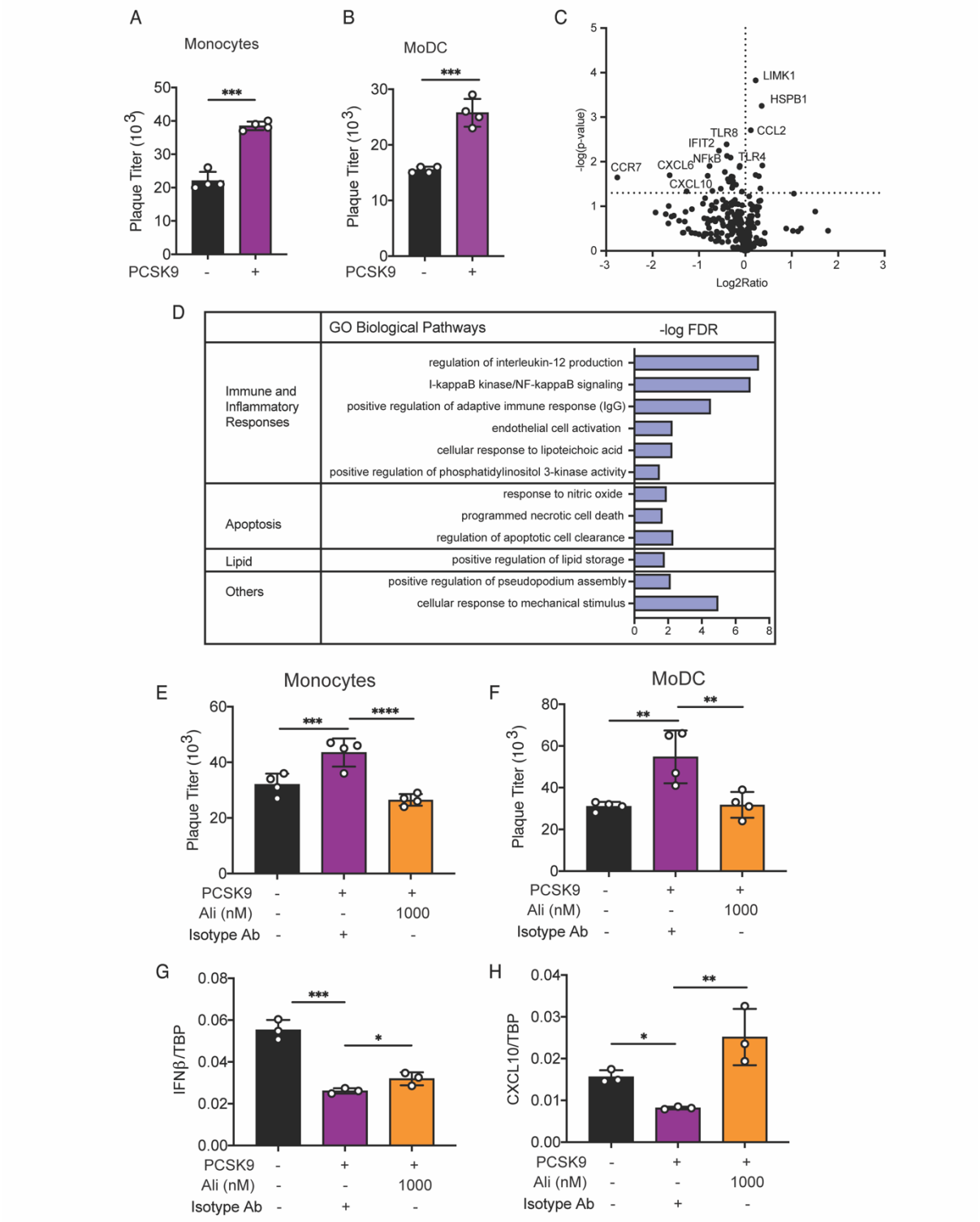

Figure 3: PCSK9 augments DENV infection in primary myeloid cells. (A) Plaque titers for hypoxic primary monocytes 48hpi with DENV. Cells were cultured without (black) or with supplementation of 400ng/ml *PCSK9* (purple) 24 hours prior to DENV2 infection. **(B)** Plaque titers for hypoxic primary monocytes derived dendritic cells 48hpi with DENV. Cells were cultured without (black) or with supplementation of 400ng/ml *PCSK9* (purple) 24 hours prior to DENV2 infection. **(C)** Volcano plot displaying 245 genes detected by nanostring in primary monocytes 24hpi with DENV2. **(D)** Pathway analysis of genes that were most abundantly downregulated in PCSK9 supplemented primary monocytes as compared to non-supplemented cells 24hpi with DENV2.

Downregulated genes were analyzed against the GO biological pathway analysis and further summarized via REVIGO. **(E)** Plaque titers of hypoxic primary monocytes 48 hours post DENV2 infection. Cells were cultured without PCSK9 (black), with supplementation of 400ng/ml PCSK9 (purple) or PCSK9 and alirocumab (orange). **(F)** Plaque titers of hypoxic primary monocyte derived dendritic cells 48 hours post DENV infection. Cells were cultured without PCSK9 (black), with supplementation of 400ng/ml *PCSK9* (purple) or *PCSK9* and alirocumab (orange). **(G-H)** mRNA expression of *IFNb* (D) and *CXCL10* (E) in hypoxic monocyte derived dendritic cells without (black) or with PCSK9 supplementation (purple) 6 hours post DENV2 infection. Experiments (A-B, E-H) were replicated 3 times, each with a minimum of 3 biological replicates. Representative data from 1 of these 3 independent experiments are shown in the Figures. Data in (A-B) was compared by unpaired t-test and (E-H) by one-way ANOVA corrected for multiple comparisons. Data in (A-B, E-H) represents mean ± SD. *P<0.05, ***P<0.001, ****P<0.0001 (unpaired t-test)

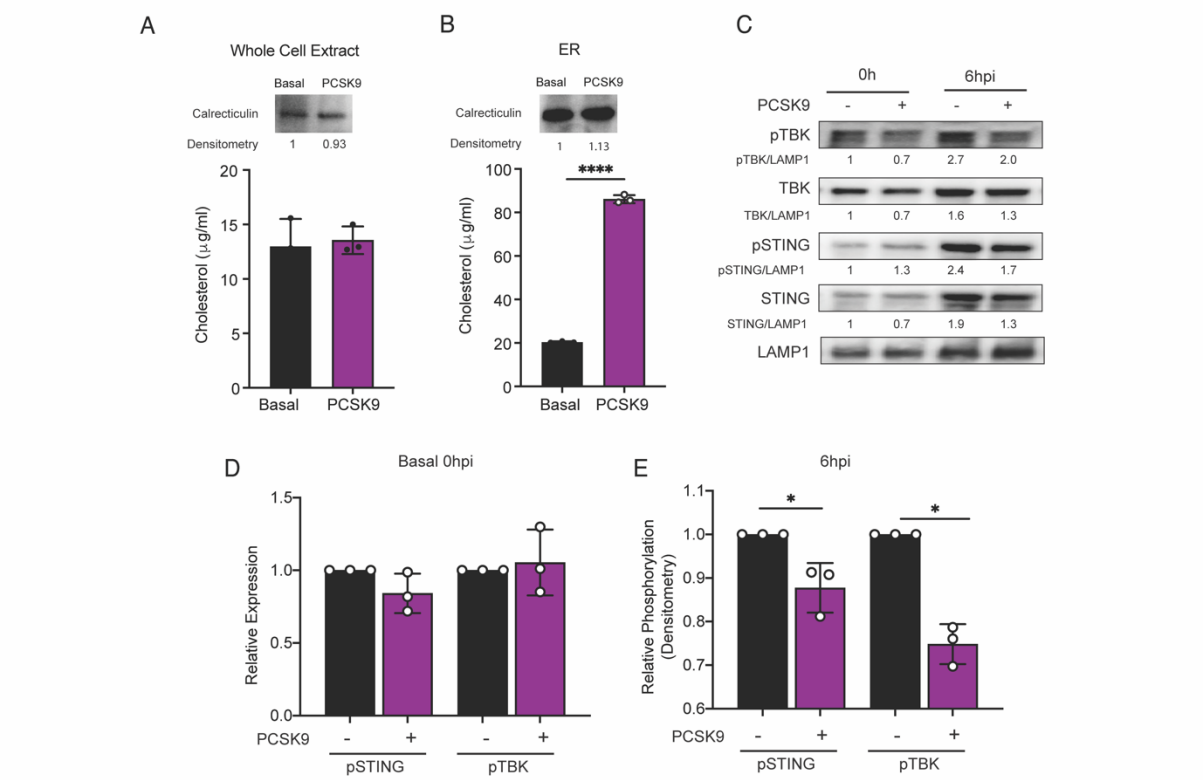

744
745 **Figure 4: PCSK9 suppresses STING-dependent induction of type-I IFN during**
746 **DENV infection. (A)** ER cholesterol quantification of whole cell extract of Huh7 cells
747 with (purple) and without (black) *PCSK9* supplementation. **(B)** ER cholesterol
748 quantification of ER organelle of Huh7 cells with (purple) and without (black) PCSK9
749 supplementation. **(C)** Representative western blot of levels of phospho-*TBK*, *TBK*,
750 phospho-*STING*, *STING* and *LAMP1* with or without *PCSK9* supplementation in
751 Huh7 cells at 0 and 6 hours post DENV2 infection. *LAMP1* served as a loading
752 control. Numbers under each western blot indicate levels of each protein normalized
753 to *LAMP1* and relative to Huh7 cells without PCSK9 supplementation at 0hpi. **(D-E)**
754 DENV infection samples in Figure 3C was repeated three times as shown by a
755 densitometry bar graph. Relative phosphorylation represents levels of each protein
756 normalized to *LAMP1* and relative to Huh7 cells without *PCSK9* supplementation 0
757 (D) and 6 (E) hours post DENV2 infection. Experiments were replicated 3 times,
758 each with a minimum of 3 biological replicates. Representative data from 1 of these
759 3 independent experiments are shown in the Figures. Data in (A-B, D-E) represents
760 mean ± SD. *P<0.05, ****P<0.0001 (unpaired t-test)

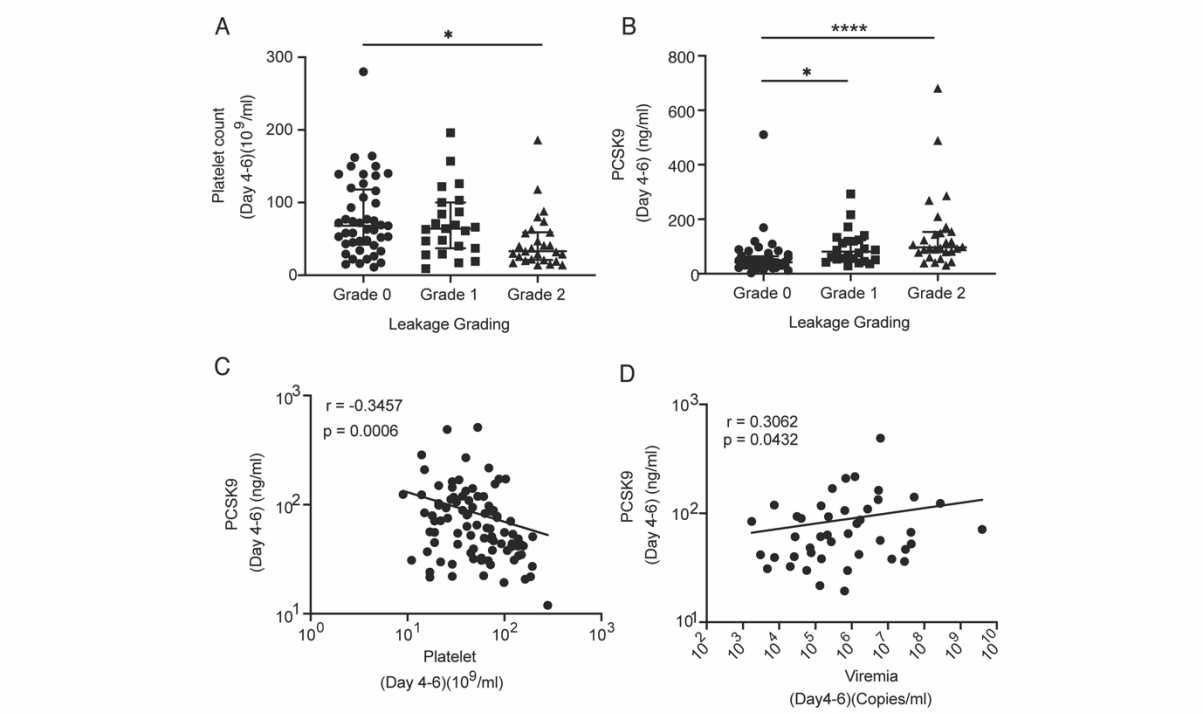

Figure 5: Increased plasma PCSK9 concentrations is associated with higher viremia, greater extent of thrombocytopenia and plasma leakage in dengue patients. (A) Platelet counts of patients 4 to 6 days post illness onset, categorized by disease severity. **(B)** PCSK9 concentrations in patients 4 to 6 days post illness onset, categorized by disease severity. **(C)** Spearman correlation of PCSK9 and platelet counts of patients 4-6 days post illness onset. Normal platelet counts in patients ranges from 150-400x10^9/L. **(D)** Spearman correlation of PCSK9 and plasma viremia levels 4-6 days post illness. Data in (A-B) was compared by one-way ANOVA corrected for multiple comparisons. Data in (A-B) represents mean ± SD. **P<0.01, ***P<0.001, ****P<0.0001 (unpaired t-test)

Supplementary Figures

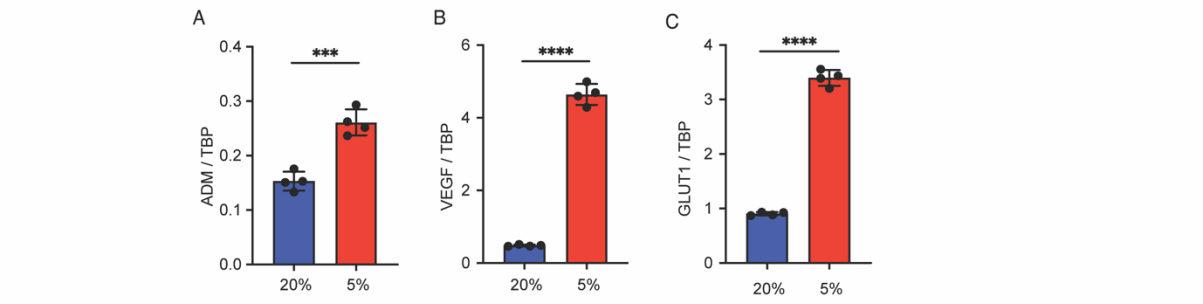

Supplementary Figure 1: Hypoxia upregulates cholesterol biosynthesis genes **(A)** *ADM* mRNA expression in normoxic (blue) or hypoxic (red) Huh7 cells 24 hours post oxygen adaptation. **(B)** *VEGF* RNA expression in normoxic (blue) or hypoxic (red) Huh7 cells 24 hours post oxygen adaptation. **(C)** *GLUT1* RNA expression in normoxic (blue) or hypoxic (red) Huh7 cells 24 hours post oxygen adaptation. Experiments were replicated 3 times, each with a minimum of 3 biological replicates. Representative data from 1 of these 3 independent experiments are shown in the Figures. Data in (A-C) represents mean ± SD. ***P<0.001, ****P<0.0001 (unpaired t-test)

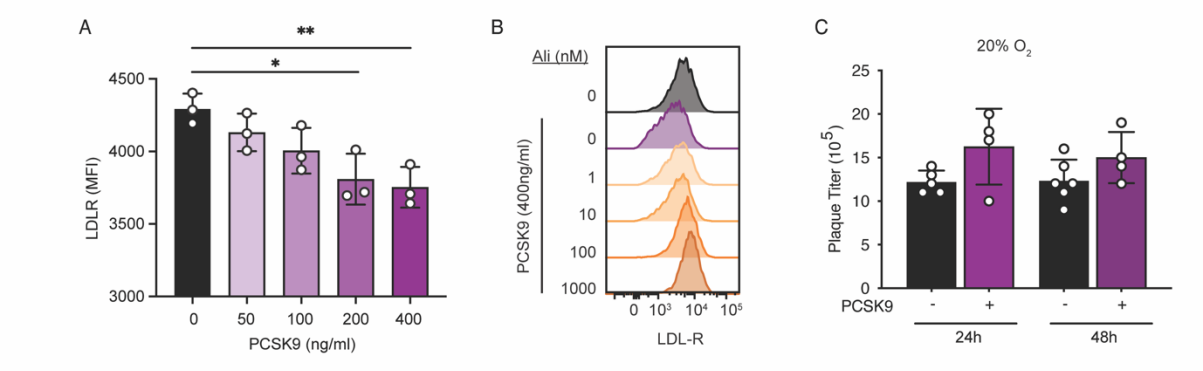

Supplementary Figure 2: PCSK9 alters LDLR expression

(A) Mean fluorescence intensity (MFI) of LDLR in hypoxic Huh7 cells supplemented with increasing concentrations of recombinant PCSK9. **(B)** Mean fluorescence intensity (MFI) of LDLR in hypoxic Huh7 cells supplemented with 400ng/ml PCSK9 and varying concentrations of alirocumab. **(C)** Plaque titers in normoxic Huh7 cells at 24 and 48hpi with or without PCSK9 supplementation. Mean fluorescence intensity (MFI) of LDLR in hypoxic Huh7 cells supplemented with 400ng/ml PCSK9 and varying concentrations of alirocumab. Experiments were replicated 3 times, each with a minimum of 3 biological replicates. Representative data from 1 of these 3 independent experiments are shown in the Figures. Data in (A and C) represents mean ± SD. *P<0.05, **P<0.01 (unpaired t-test)

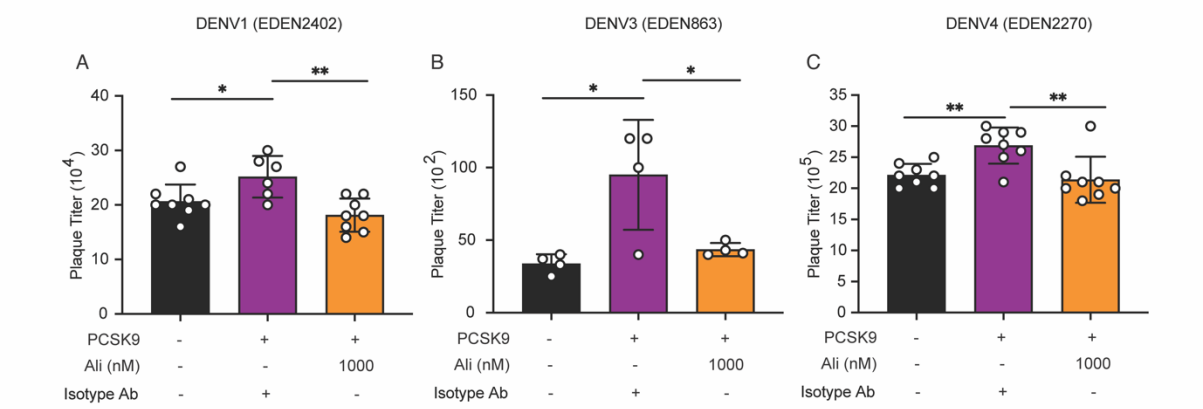

Supplementary Figure 3: PCSK9 alters DENV infection of different serotypes

(A-C) Plaque titers in hypoxic Huh7 cells 48 hours post-infection with DENV1 (A), DENV3 (B) and DENV4 (C). Cells were cultured without (black), with supplementation of 400ng/ml *PCSK9* (purple) or PCKS9 with alirocumab (orange) for 24 hours prior to DENV infection. Experiments were replicated 3 times, each with a minimum of 3 biological replicates. Representative data from 1 of these 3 independent experiments are shown in the Figures. Data in (A-C) represents mean ± SD. *P<0.05, **P<0.01 (unpaired t-test)

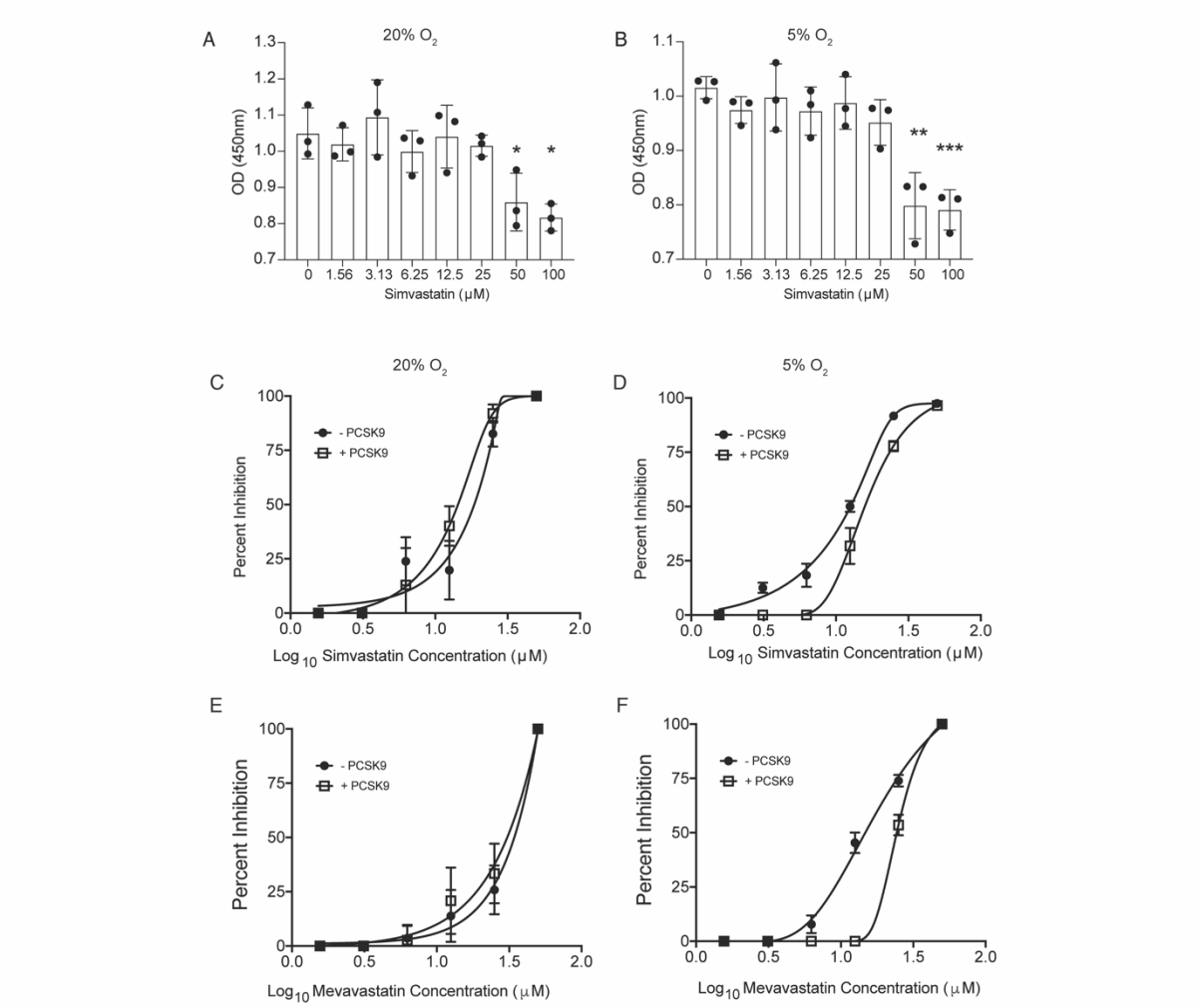

Supplementary Figure 4: PCSK9 alters antiviral activity of statins under hypoxic conditions. (A-B) MTS OD values of normoxic (A) and hypoxic (B) Huh7 48 hours post simvastatin treatment. **(C-D**) Dose response curves for EC50 analysis of normoxic (C) and hypoxic (D) Huh7 cells 48hpi with DENV2 treated with varying doses of simvastatin, with or without PCSK9 supplementation. **(E-F**) Dose response curves for EC50 analysis of normoxic (E) and hypoxic (F) Huh7 cells 48hpi with DENV2 treated with varying doses of mevastatin, with or without PCSK9 supplementation. Experiments were replicated 3 times, each with a minimum of 3 biological replicates. Representative data from 1 of these 3 independent experiments are shown in the Figures. Data in (A-B) represents mean ± SD. *P<0.05, ***P<0.001, ***P<0.001 (unpaired t-test)

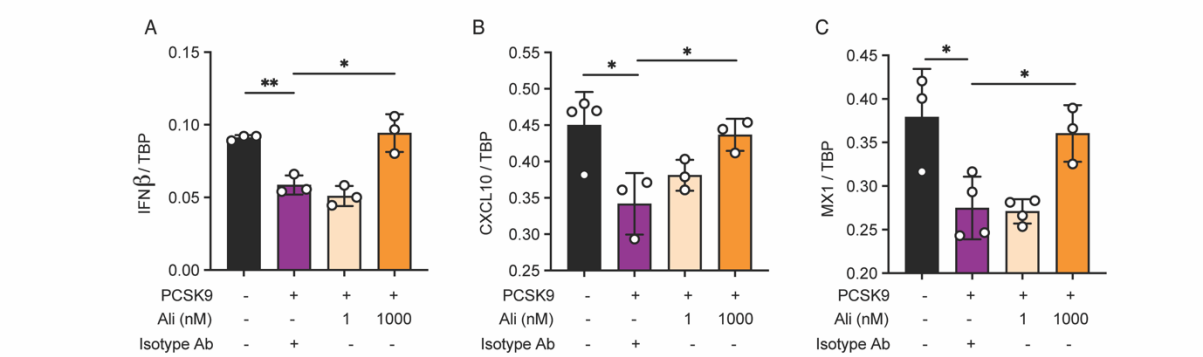

Supplementary Figure 5: PCSK9 suppresses induction of type-I IFN during DENV infection. **(A-C)** mRNA expression of *IFNb* (A), *CXCL10* (B) and *MX1* (C) in hypoxic Huh7 cells without (black) or with PCSK9 supplementation (purple) 6 hours post DENV2 infection. Cells were with increasing doses of alirocumab (orange) for 24 hours prior to DENV2 infection. Experiments were replicated 3 times, each with a minimum of 3 biological replicates. Representative data from 1 of these 3 independent experiments are shown in the Figures. Data in (A-C) represents mean ± SD. *P<0.05, **P<0.01 (unpaired t-test)

825 Table 1: Characteristics of patients in the clinical cohort

			Plasma Leakage Grading					
Characteristic	**No.**	**All Patients (n=111)**	**No.**	**Grade 0 (n=53)**	**No.**	**Grade 1 (n=27)**	**No.**	**Grade 2 (n=29)**
Age	111	23 (14 – 31)	55	26 (21 – 34)	27	27 (19 – 36)	29	11 (8 – 17.50)
Male	111	53 (47.74%)	55	27 (50.93%)	27	14 (51.85%)	29	14 (48.28%)
Hospitalized	111	102 (91.89%)	55	47 (85.45%)	27	26 (96.30%)	29	29 (100%)
DENV PCR Positive	111	75 (68.80%)	55	37 (69.81%)	27	22 (81.48%)	29	16 (55.17%)
Hospitalized	111	102 (93.58%)	55	47 (88.68%)	27	26 (96.3%)	29	29 (100%)
WHO Severity	111		55		27		29	
Mild Dengue		30 (27.03%)		26 (47.27%)		4 (14.82%)		0 (0%)
WS		59 (53.32%)		29 (52.73%)		22 (81.48%)		8 (27.59%)
Severe		22 (19.82%)		0 (0%)		1 (3.70%)		21 (72.41%)
Serology	111		55		27		29	
Undetermined		40 (36.04%)		24 (43.64%)		6 (22.22%)		10 (34.48%)
Primary		12 (10.81%)		6 (10.91%)		5 (18.52%)		1 (3.45%)
Secondary		59 (53.15%)		25 (45.45%)		16 (59.26%)		18 (62.07%)
Serotype	111		55		27		29	
Undetermined		35 (31.53%)		18 (32.73%)		4 (14.81%)		13 (44.83%)
1		26 (23.42%)		9 (16.36%)		7 (25.93%)		10 (34.48%)
2		14 (12.61%)		7 (12.73%)		4 (14.81%)		3 (10.34%)
3		20 (18.02%)		12 (21.82%)		8 (29.63%)		0 (0%)
4		16 (14.41%)		9 (16.36%)		4 (14.81%)		3 (10.34%)

826
827 Summary statistics are absolute counts (%) for categorical variables and median (interquartile range) for continuous data.

828 Table 2: Laboratory parameters of the patients by illness phase

			Plasma Leakage Grading						Grade 1 v 0	Grade 2 v 0
Units	No.	All Patients (n=109)	No.	Grade 0 (n=53)	No.	Grade 1 (n=27)	No.	Grade 2 (n=29)	p-value	p-value
Platelets, 10^9/L										
Days 1-3	42	143 (77.75 – 177)	25	150 (92 – 186.5)	11	117 (64 – 175)	6	89 (21 – 158)	0.8376	0.1993
Days 4-6	95	58 (29 – 88)	45	68 (42 – 118)	23	64 (37 – 100)	27	33 (21 – 59)	0.7781	**0.0127**
Days 7-10	28	62 (38.25 – 97)	15	90 (43 – 135)	7	38 (25 – 78)	6	57 (38.75 – 64.75)	0.2367	0.2996
Day 11-28	26	313.5 (255.3 – 345.3)	8	276 (219.3 – 361.8)	9	321 (257.5 – 361.5)	9	310 (280.5 – 345.5)	0.2969	0.8795
WBC, 10^9/L										
Days 1-3	44	4.330 (3.05 – 5.6)	25	4.5 (3.45 – 5.8)	13	4 (2.15 – 4.7)	6	4.6 (3.2 – 6.2)	0.2748	0.9241
Days 4-6	94	3.95 (2.5 – 5.9)	44	4 (2.5 – 5.2)	23	2.5 (1.7 – 3.9)	27	7 (4 – 8.9)	0.0848	**0.0003**
Days 7-10	28	4.7 (3.55 – 5.98)	15	5.1 (3.7 – 6.1)	7	3.8 (2.6 – 8)	6	4.2 (3.63 – 7.3)	0.8585	0.9845
Day 11-28	26	6.5 (5.4 – 7.6)	8	5.45 (4.7 – 6.1)	9	6.6 (5.35 – 7.65)	9	7.34 (6.47 – 8.58)	0.3592	**0.0161**
Neutrophil (% of WBC)										
Days 1-3	42	61.35 (52.53 – 74.85)	24	63 (55.3 – 76.35)	13	61.70 (49.9 – 72.15)	5	52.70 (19.8 – 61.65)	0.8802	0.0889
Days 4-6	94	40.1 (29.35 – 51.38)	45	37.6 (25.15 – 50.9)	23	42.8 (35.2 – 58.3)	26	41.5 (29.43 – 49.8)	0.1625	0.9115
Days 7-10	28	36.35 (31.45 – 49.65)	15	35 (28.5 – 47.7)	7	36 (30.9 – 44.5)	6	47.3 (34.88 – 52.83)	0.7969	0.5504
Day 11-28	26	47.95 (43.05 – 52.9)	8	50 (46.2 – 56.35)	9	46.8 (43.65 – 53.25)	9	41.9 (39.1 – 50.7)	0.8586	0.1358
Lymphocyte (% of WBC)										
Days 1-3	44	22.55 (18.78)	25	22.1 (16.8 – 30.35)	13	22.9 (14.3 – 29.45)	6	25.8 (19.15 – 64.7)	0.9381	0.1252
Days 4-6	95	43.1 (29.2 – 53.5)	45	43.7 (32.1 – 58.1)	23	39.5 (25.4 – 52.8)	27	40.6 (30.1 – 49.9)	0.2675	0.5350
Days 7-10	28	42.8 (31.5 – 49.8)	15	43.2 (34.5 – 51.5)	7	37.9 (34.7 – 44.1)	6	37.1 (27.45 – 48.5)	0.9959	0.8071
Day 11-28	26	38.4 (24.75 – 42.45)	8	35.55 (29.35 – 39.2)	9	38.6 (33.3 – 43.15)	9	41.3 (38 – 46.05)	0.5094	**0.0223**
AST (U/L)										
Days 1-3	33	31 (24 – 58.5)	18	27 (17.5 – 34)	10	47 (30 – 106.3)	5	42 (28.5 – 572.5)	0.3845	**0.0037**
Days 4-6	43	105 (63 – 142)	18	63.5 (30.75 – 100.5)	7	118 (73 – 352)	18	127 (107 – 226)	**0.0470**	**0.0327**
Days 7-10	4	114.5 (36 – 513.3)	1	26	1	163	2	348 (66 – 630)	-	-
Day 11-28	13	29 (21 – 42)	5	24 (21- 35.5)	7	39 (23 – 46)	1	17	0.3675	-
ALT (U/L)										
Days 1-3	34	19 (12 – 32.5)	18	17 (11 – 20.5)	11	29 (16 – 76)	5	32 (12.5 – 220)	0.2209	**0.0077**
Days 4-6	43	48 (31 – 81)	18	45 (19.25 – 69.75)	7	47 (28 – 289)	18	59 (34 – 89.25)	0.7551	0.5499
Days 7-10	4	62.5 (43.5 – 154.3)	1	42	1	77	2	114 (48 – 180)	-	-
Day 11-28	13	38 (24 – 73.5)	5	30 (18 – 53)	7	60 (38 – 82)	1	8	0.1158	-
PCSK9 (ng/ml)										
Days 1-3	43	55.98 (36.88 – 85.66)	24	46.52 (29.67 – 76.40)	13	69.32 (40.04 – 98.64)	6	68.98 (66.02 – 184.1)	0.5264	0.0547
Days 4-6	98	60.47 (39.11 – 109.8)	46	41.62 (30.80 – 63.56)	24	81.31 (51.53 – 122.9)	28	96.54 (78.78 – 153.5)	**0.0426**	**<0.0001**
Days 7-10	28	77.58 (33.17 – 89.06)	15	62 (27.16 – 79.38)	7	84.99 (33.25 – 244.1)	6	88.27 (66.46 – 121.6)	0.0609	0.5605

Day 11-28	29	21.3 (12.07 – 28.17)	9	21.41 (13.42 – 25.37)	9	19.80 (10.56 – 50.21)	11	21.30 (12.07 – 28.17)	0.2969	0.8795
Viremia (copies/ml)										
Days 1-3	31	$1.32x10^8$ ($2.28x10^6$ – $1.17x10^9$)	16	$8.58x10^7$ ($2.74x10^6$ – $5x10^8$)	11	$5.91x10^8$ ($3.17x10^7$- $4.08x10^9$)	4	$2.04x10^6$ ($1.03x10^6$ – $6.97x10^9$)	0.1596	0.1488
Days 4-6	43	$6.34x10^5$ ($5.73x10^4$ – $5.33x10^6$)	21	$1.46x10^5$ ($2.32x10^4$ – $1.77x10^6$)	10	$3x10^6$ ($9.57x10^5$ – $3.22x10^7$)	12	$4.58x10^5$ ($6.61x10^4$ – $4.47x10^6$)	0.7877	0.3847

Summary statistics are absolute counts (%) for categorical variables and median (interquartile range) for continuous data. Comparative analysis was performed by one-way ANOVA. Numbers in bold represent statistically significant comparisons. Abbreviations: WBC – white blood cell count, AST – aspartate aminotransferase, ALT – alanine aminotransferase, PCSK9 – proprotein convertase subtilisin/kexin type 9.